Since January 2020 Elsevier has created a COVID-19 resource centre with free information in English and Mandarin on the novel coronavirus COVID-19. The COVID-19 resource centre is hosted on Elsevier Connect, the company's public news and information website.

VIROLOGY 166, 66–75 (1988)

Synthesis of Virus-Specific RNA in Permeabilized Murine Coronavirus-Infected Cells

JULIAN L. LEIBOWITZ[1] AND JAMES R. DEVRIES

Department of Pathology and Laboratory Medicine, P.O. Box 20708, University of Texas Health Science Center, Houston, Texas 77225

Received December 29, 1987; accepted May 3, 1988

We have developed a permeabilized cell system for assaying mouse hepatitis virus-specific RNA polymerase activity. This activity was characterized as to its requirements for mono- and divalent cations, requirements for an exogenous energy source, and pH optimum. This system faithfully reflects MHV-specific RNA synthesis in the intact cell, with regard to both its time of appearance during the course of infection and the products synthesized. The system is efficient and the RNA products were identical to those observed in intact MHV-infected cells as judged by agarose gel electrophoresis and hybridization. Permeabilized cells appear to be an ideal system for studying coronavirus RNA synthesis since they closely mimic *in vivo* conditions while allowing much of the experimental flexibility of truly cell-free systems.

INTRODUCTION

The coronaviruses comprise a group of large enveloped positive-strand viruses with a unique replication scheme. The genomic RNA is about 27 kb in size (Boursnell *et al.*, 1987) and shares many structural features with the genomes of other positive-strand viruses, i.e., it is capped at the 5′ terminus (Lai *et al.*, 1982a), is polyadenylated at the 3′ end (Lomniczi, 1977; Yogo *et al.*, 1977), and can function as messenger RNA *in vitro* (Leibowitz *et al.*, 1982; Denison and Perlman, 1986) and presumably *in vivo* as well (Denison and Perlman, 1987). The translation product(s) of the virion RNA is hypothesized to include the coronavirus-specific RNA-dependent RNA polymerase, although this has never been rigorously demonstrated.

In addition to the virion RNA, infected cells contain several other classes of coronavirus-specific RNA (Stern and Kennedy, 1980a; Lai *et al.*, 1981; Leibowitz *et al.*, 1981; Spaan *et al.*, 1981). Lai and co-workers have demonstrated that MHV-infected cells contain a single RNA species of negative polarity which is genome length (1982b). This negative-strand RNA is thought to serve as the template for positive-strand mRNA synthesis. For mouse hepatitis virus (MHV), one of the most extensively studied coronaviruses, there are seven species of MHV-specific mRNA present in infected cells, the largest of which is indistinguishable from virion RNA (Leibowitz *et al.*, 1981; Lai *et al.*, 1981; Spaan *et al.*, 1981). Structural analyses of these RNAs have shown them to make up a "nested set" with coterminal 3′ ends (Leibowitz *et al.*, 1981; Stern and Kennedy, 1980a,b; Lai *et al.*, 1981; Cheley *et al.*, 1981; Weiss and Leibowitz, 1983; Spaan *et al.*, 1982). A unique feature of coronavirus replication is the presence of a common leader sequence of about 70 bases at the 5′ end of each message which is present only once (at the 5′ end) in the virion RNA (Spaan *et al.*, 1983; Lai *et al.*, 1983, 1984; Baric *et al.*, 1985). The mechanism of synthesis of all species of coronavirus-specific RNAs is largely unknown.

Progress in studying the details of the synthesis of the MHV mRNAs has been hampered somewhat by the lack of an efficient and easily reproducible *in vitro* transcription system which faithfully reproduces the events which occur in intact cells. Several groups of workers have demonstrated actinomycin D-resistant RNA polymerase activity in extracts of coronavirus-infected cells. Dennis and Brian (1982) have reported the presence of a membrane-associated polymerase activity in cytoplasmic extracts of TGEV-infected cells. A similar activity has been demonstrated to be present in extracts of MHV-infected cells (Brayton *et al.*, 1982, 1984; Mahey *et al.*, 1983). Recently, Compton *et al.* (1987) have described a system based on an extract from lysolecithin-treated cells. These systems have either been difficult to work with due to their relatively low efficiencies, or they have been hard to reproduce and maintain on a daily basis, or they do not faithfully reflect the pattern of MHV RNA synthesis observed in infected cells.

To circumvent the short-comings of the existing *in vitro* MHV polymerase systems and to overcome the relative experimental limitations of intact cells, we have taken an approach similar to that used by Condra and Lazzarini (1980) for studying VSV replication. In this paper we report the characteristics of a permeabilized cell system and demonstrate that it incorporates ribonucle-

[1] To whom requests for reprints should be addressed.

0042-6822/88 $3.00

otide triphosphates into RNA molecules which appear identical to the virus-specific mRNAs synthesized in MHV-infected cells.

MATERIALS AND METHODS

Cells and virus

Monolayer cultures of 17CL-1 cells were grown as described previously (Sturman and Takemoto, 1972; Leibowitz *et al.*, 1981). The origin and growth of the A59 (MHV-A59) and JHM (MHV-JHM) strains of mouse hepatitis virus have been described (Robb and Bond, 1979).

Permeabilization of cells and radioactive labeling

Monolayer cultures of 17Cl-1 cells were trypsinized and infected in suspension as described previously (Robb and Bond, 1979) at a multiplicity of infection equal to 3 PFU per cell. Infected or mock-infected cells were plated in 35-mm 6-well cluster dishes (Costar) at 2×10^6 cells/well in Dulbecco's modified Eagle's medium (DME) containing 2% fetal bovine serum and incubated at 37°. At 3 hr postinfection actinomycin D (Sigma) was added to the cultures at 10 μg/ml to inhibit host DNA-dependent RNA synthesis. At the times indicated for each individual experiment, the dishes were placed on ice and washed twice with serum-free DME. Buffer A [50 m*M* Tris, pH 8.0, 4.5 m*M* $MgAc_2$, 20 m*M* KCl, 5 m*M* NaCl, 150 m*M* RNase-free sucrose (Swartz/Mann Biotech)] was then added to the cultures. For our standard permeabilization conditions, synthetic lysolecithin (L-*d*-lysophosphatidylcholine, palmitoyl, Sigma) was added to a concentration of 150 μg/ml and the cells were held on ice for 90 sec. Lysolecithin was removed from the cultures by aspirating the buffer followed by one wash with buffer A without lysolecithin. Buffer B was then added to the cultures and the cells were incubated at 37°. The make up of buffer B varied, as described under Results, over the course of the work reported here. In our initial experiments buffer B contained 30 m*M* Tris, pH 8.0, 33 m*M* NH_4Cl, 5 m*M* NaCl, 20 m*M* KCl, 4.5 m*M* $MgAc_2$, 200 μ*M* each GTP, ATP, and CTP (Pharmacia), 12 μ*M* creatine phosphate (Sigma), 200 μ*M* spermidine trihydrochloride (Sigma), 10 μ*M* dTTP (Pharmacia), 100 μg/ml creatine phosphokinase (75 units/mg, bovine heart, Sigma Type III), 1 m*M* dithiothreitol (Research Organics), 150 m*M* RNase-free sucrose, 10 μg/ml actinomycin D. [^{3}H]UTP (ICN, 30 Ci/mmol) was added at 25 μCi/ml to a concentration of 1.8 μ*M*. Experiments to optimize polymerase activity led to the following standard concentrations for buffer B (final pH of 8.0): 30 m*M* Tris, pH 8.0, 44 m*M* NaCl, 20 m*M* KCl, 6 m*M* $MgAc_2$, 1 m*M* ATP, 200 μ*M* GTP, 200 μ*M* UTP, 2.5 μ*M* of unlabeled CTP, 12 μ*M* creatine phosphate, 200 μ*M* spermidine, 10 μ*M* dTTP, 100 μg/ml creatine phosphokinase, 1 m*M* dithiothreitol, 150 m*M* sucrose, 10 μg/ml actinomycin D, 0.24 TIU/ml aprotinin (Sigma), 20 ng/ml ouabain octahydrate (Sigma). [^{3}H]CTP (ICN) was added at 62.5 μCi/ml yielding a final CTP concentration of 4.5 μ*M*. Following incubation at 37° for the indicated times (40 min for most experiments), the reaction was stopped by the addition of an equal volume of 2% sodium dodecyl sulfate (Sigma) to the cultures.

Polymerase activity was assayed by precipitating labeled RNA from replicate cultures by the addition of trichloroacetic acid (TCA) containing 1% sodium pyrophosphate (Sigma) to a final concentration of 5%. TCA-insoluble precipitates were collected on glass fiber filters and extensively washed with 5% TCA, and the TCA-precipitable radioactivity was quantitated by liquid scintillation counting.

Extraction and electrophoresis of RNA

RNA was extracted from cell cultures and permeabilized cells as described (Wittek *et al.*, 1984; Cabirac *et al.*, 1986). The cells were dissolved in 8 *M* guanidium hydrochloride, 0.1 *M* 2-mercaptoethanol, and 0.2 *M* sodium acetate, pH 5.0, and the DNA was sheared by passage through a hypodermic needle. The RNA was selectively precipitated overnight by the addition of ethanol to a concentration of 33%. The precipitated RNA was collected by centrifugation and dissolved in 50 m*M* sodium acetate, pH 5.2, 10 m*M* EDTA, 1% SDS, 1 mg/ml proteinase K and digested at 37° for 1 hr. After phenol extraction the RNA was ethanol precipitated and collected by centrifugation prior to further analysis. RNA to be analyzed by gel electrophoresis was dissolved in a buffer containing 50% formamide, 4% formaldehyde, 20 m*M* Mops [3-(*N*-morpholino)propane sulfonic acid), 5 m*M* sodium acetate, 1 m*M* EDTA, pH 7.0, and electrophoresed in 0.8% agarose gels containing formaldehyde (Lerach *et al.*, 1977).

Plasmids

The plasmids used in this work include g344 (kindly provided by Dr. Susan Weiss, University of Pennsylvania), a cDNA clone of MHV-A59 which encompasses a portion of gene 7 all of genes 5 and 6, and the 3′ portion of gene 4 (Budzilowicz *et al.*, 1985). Previously undescribed molecular clones of MHV-JHM used in this work are 118-8a, a cDNA clone which extends from the 3′ poly(A) of the genome to position 119 in gene 7, a distance of 1648 bases (Spaan *et al.*, 1983); 370-1, a cDNA clone extending from the *Pvu*II site at position 1044 of gene 7 (Spaan *et al.* 1983) to the *Pst*I site at

position 2589 of gene 3 (Schmidt *et al.,* 1987), a distance of almost 4.05 kbp; 414-8a, which extends from nucleotide 2350 to nucleotide 199 in gene 3 (Schmidt *et al.,* 1987); and 478-38a, a clone which extends from the *Dde*I site at position 350 in gene 3 into MHV gene 2 for an additional 1.8 kbp. A molecular clone representing the *Bam*HI fragment K (5.9 kbp) of the leporipoxvirus malignant rabbit fibroma virus (Strayer *et al.,* 1983a,b) was used as a control for some experiments.

Southern blot hybridization

Plasmids were digested with the appropriate restriction enzyme according to the manufacturer's suggested conditions. The resulting digests were electrophoresed in a 1% agarose gel and transferred to nitrocellulose as described previously (Southern, 1975). Nitrocellulose filters were probed either with random-primed cDNA prepared with [^{32}P]dCTP using purified MHV-A59 virion RNA as template (Weiss and Leibowitz, 1983) or with the permeabilized cell reaction products. Hybridization was performed at 42° in 50% formamide, 3× SSPE, 5× Denhardt's. The filters were washed twice in 0.1× SSPE, 1% SDS at 20° and then washed four additional times in the same buffer at 50°.

RESULTS

Standardization of permeabilization and polymerase reaction conditions

Our initial experiments were geared toward determining the optimal conditions for permeabilizing MHV-infected 17CL-1 cells. Cells were infected with MHV-A59 or mock-infected and incubated until approximately 60% of the cells were involved in syncytia. For the experiments reported here this was usually between 8.5 and 9.5 hr postinfection, a time when MHV-specific RNA synthesis was maximal. At this time the cells were washed as described under Materials and Methods and permeabilized in buffer A containing lysolecithin which was varied in concentration from 20 to 250 μg/ml. After permeabilization the cells were stained with trypan blue to determine the percentage of cells which had been made permeable to the dye at each lysolecithin concentration. These preliminary experiments demonstrated that a lysolecithin concentration of 150 μg/ml permeabilized virtually all of the MHV-infected cells and greater than 95% of the uninfected cells without making the cells too fragile to withstand the subsequent incubations. Higher concentrations of lysolecithin impaired our ability to subsequently maintain the cells for the polymerase reaction (data not shown). Our standard permeabilization conditions were therefore set at 150 μg/ml lysolecithin.

Once the conditions for permeabilization were established, we investigated the ability of permeabilized cells, in the presence of actinomycin D, to incorporate labeled precursors into TCA-precipitable material. These initial experiments were performed at a pH of 8.0, 4.5 m*M* Mg^{2+}, 5 m*M* Na^{+}, 20 m*M* K^{+}, and 33 m*M* NH_4^{+}. These conditions were based upon those used by Brayton *et al.* (1982) in a cell-free MHV polymerase system. Permeabilized cells were incubated with [^{3}H]UTP or [^{3}H]CTP in the presence of the three other unlabeled ribonucleotide triphosphates, actinomycin D, and an energy regenerating system, in buffer B. The amount of TCA-precipitable radioactivity was several-fold greater in MHV-infected cells than in mock-infected controls (data not shown). The synthesis of radioactivity labeled material from labeled ribonucleotide triphosphates required permeabilization; cells in which the lysolecithin treatment was omitted did not incorporate any radioactivity (Table 1). The TCA-precipitable material synthesized in permeabilized cells was demonstrated to be RNA in subsequent experiments on the basis of it being completely sensitive to RNase digestion and completely resistant to digestion with DNase (Table 2).

The ability of permeabilized, MHV-infected cells to incorporate [α-^{32}P]CTP into acid-precipitable material

TABLE 1

CHARACTERIZATION OF MHV RNA POLYMERASE ACTIVITY IN PERMEABILIZED CELLS

Reaction conditions	Percentage activity present under control reaction conditions[a]
−Permeabilization	0
−Spermidine	66
−Creatine phosphokinase and creatine phosphate	51
−Mg^{2+}	19
−Mg^{2+}, +Mn^{2+} (6 m*M*)	11
−Mg^{2+}, +Ca^{2+} (5, 10, or 20 m*M*)	0
−GTP	17
−UTP	2
−UTP, −GTP	6
+50 μ*M* PMSF[b]	78
+Aprotinin[b]	121
+40 units/ml RNasin[b]	106
+Ouabain, 1 ng/ml[c]	125
+Ouabain, 20 ng/ml[c]	131

[a] The results of several different experiments are summarized. All data are presented as a percentage of the activity obtained in appropriate control polymerase reactions in permeabilized cells. Precise reaction conditions for the experiments varying divalent cations are given in the legend of Fig. 2. All other reactions were performed under the standard cation conditions as discussed in the text.

[b] Performed in the absence of inhibitors other than actinomycin D.

[c] Performed in the presence of aprotinin.

TABLE 2

EFFECT OF RNase AND DNase DIGESTION ON TCA-PRECIPITABLE MATERIAL SYNTHESIZED IN PERMEABILIZED CELLS

Source of material digested	Treatment		
	None	RNase[a]	DNase[b]
Permeabilized cells[c]			
Mock-infected	1,198	20	1,220
MHV-infected	7,881	29	8,110
In vivo labeled cells[d]			
Mock-infected	596	33	609
MHV-infected	109,000	90	109,500

[a] Samples corresponding to the amount of RNA present in a 35-mm well (for permeabilized cells) or a 100-mm tissue culture dish (*in vivo* labeled cells) were digested with 100 μg RNase A and 10 μg RNase T1 for 60 min at 37° and TCA precipitated in the presence of carrier tRNA.

[b] Samples identical to those digested with RNase were digested with RNase-free DNase 1 (Promega) for 60 min at 37°.

[c] Infected and uninfected cells were permeabilized at 8 hr postinfection, labeled with [^{32}P]CTP and the cellular RNA was extracted as described under Materials and Methods.

[d] Infected and uninfected cells were labeled with 100 μCi/ml [^{3}H]uridine in the presence of actinomycin D and the RNA was extracted.

was dependent upon adding an excess of ATP as compared to the three other ribonucleotide triphosphates. An ATP concentration of 1.0 m*M* achieved the best results. Higher levels of ATP made the permeabilized cells extremely fragile and inhibited incorporation (data not shown).

Previous investigators using cell-free systems had demonstrated pH optima for MHV-specific RNA-dependent RNA polymerase activity at 8.4, 8.0, or 7.4, depending upon the system used. To determine the optimum pH for measuring MHV-specific polymerase activity in permeabilized cells, infected and mock-infected cells were permeabilized and assayed for polymerase activity as described above, with the exception that the pH of buffers A and B was varied between 7.0 and 8.4 among replicate cultures. In this assay, incorporation of labeled substrate in the presence of actinomycin D into TCA-precipitable material increased as the pH was raised from 7.0 to 8.4 (Fig. 1). The increase of polymerase activity as the pH was raised proceeded in a step-wise fashion, with the greatest increment in activity occurring as the pH was increased from 7.2 to 7.4. Further increases in the pH from 7.4 to 8.4 had a relatively small effect upon the activity, with the greatest portion of that increase occurring as the pH was changed from 7.6 to 8.0. The ability of permeabilized cells to synthesize actinomycin D-resistant RNA remained almost constant as the pH was varied from 8.0 to 8.4. Therefore we adopted pH 8.0 for our standard reaction conditions.

The magnesium requirement of MHV RNA synthesis in permeabilized cells was then determined. Infected and mock-infected cells were permeabilized at pH 8.0 and the magnesium concentration was varied from 0 to 9 m*M* in replicate cultures. As can be seen in Fig. 2 and in Table 1, there was a strict requirement for Mg^{2+} in this system. In the absence of Mg^{2+} the polymerase activity was reduced to 19% of the amount observed at 6.0 m*M* Mg^{2+}. Although Mg^{2+} was needed for measuring the MHV polymerase activity in permeabilized cells the optimum was rather broad. The requirement for magnesium cannot be replaced by either Mn^{2+} or Ca^{2+} (Table 1), both of which resulted in less activity than that obtained when magnesium was simply omitted from the reaction mix. A magnesium concentration of 6.0 m*M* was chosen for our standard reaction conditions.

To further optimize the system we next investigated the monovalent cation requirements of the MHV polymerase/permeabilized cell system. Infected and mock-infected cells were permeabilized as described above, except that the pH and magnesium concentration were held constant at 8.0 and 6.0 m*M*, respectively, and the Na^{+}, K^{+}, and NH_4^{+} concentrations were varied as described below. Initial experiments determined that K^{+} and NH_4^{+} seemed to be interchangeable in this sys-

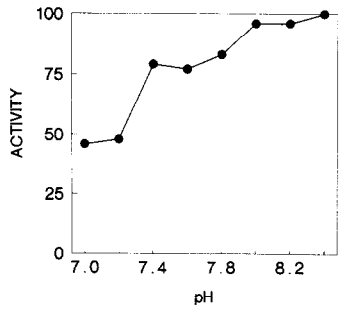

FIG. 1. Determination of pH optimum for MHV RNA polymerase activity in permeabilized cells. Cells were infected with MHV-A59 at a m.o.i. of 3, or mock-infected, and incubated until 8.5 hr postinfection. The cells were permeabilized as described under Materials and Methods. Replicate cultures were assayed for MHV RNA polymerase activity using the original formulation of buffer B (33 m*M* NH_4Cl, 5 m*M* NaCl, 20 m*M* KCl, 4.5 m*M* $MgCl_2$, as described under Materials and Methods with the exception that the pH was varied between 7.0 and 8.4 among the replicate cultures. After 40 min of incubation the assay was terminated and the amount of radioactivity incorporated into TCA-precipitable material was determined. All data points represent the mean of duplicate samples. The results were calculated by subtracting the amount of radioactivity in mock-infected samples from that incorporated into MHV-infected samples under identical conditions. The results are expressed in arbitrary units with the maximum activity being set at 100.

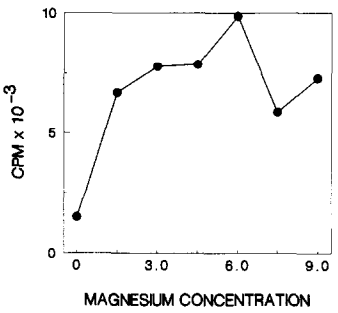

FIG. 2. Determination of the magnesium optimum for MHV RNA polymerase activity in permeabilized cells. Cells were infected with MHV-A59 or mock-infected and incubated until 9 hr postinfection. The cells were permeabilized and incubated in a formulation of buffer B which contained 30 m*M* Tris, 33 m*M* NH_4Cl, 5 m*M* NaCl, 20 m*M* KCl, pH 8.0, as described under Materials and Methods with the exception that the magnesium concentration was varied between 0 and 9 m*M* among replicate cultures. At 40 min incubation the assay was terminated and the amount of radioactivity incorporated into TCA-precipitable material was determined. All data points represent the mean of duplicate samples. The results were calculated by subtracting the amount of radioactivity in mock-infected samples from that incorporated into MHV-infected samples under identical conditions.

tem, Na^+ was required for activity, and a total monovalent cation concentration greater than 80 m*M* resulted in a decrease in polymerase activity (data not shown). The MHV polymerase activity present in permeabilized cells was relatively insensitive to monovalent cation concentrations, as long as the total monovalent cation remained below 80 m*M*. K^+ was not required; the omission of K^+ from buffer B decreased activity by 5–10%. At concentrations above 80 m*M* $Na^+ + K^+$ the polymerase activity decreased somewhat. We adopted final concentrations of 44 m*M* Na^+ and 20 m*M* K^+ in buffer B for our standard reaction conditions. These concentrations were convenient to use and approximately in the center of the broad optimum concentrations of monovalent cations.

The requirements of the MHV polymerase/permeabilized cell system for various cofactors were determined. As shown in Table 1, the omission of spermidine decreased the activity to 66% of that observed with the complete system. There was a requirement for an energy regenerating system; the omission of CPK and creatine phosphate decreased activity to 51% of control values. The system also required all four ribonucleotide triphosphates. The omission of either GTP or UTP decreased incorporation of labeled CTP by 83 and 98%, respectively. The omission of both UTP and GTP decreased synthesis by 94% of that observed in the complete system. These results suggested that the activity we were detecting was not a polynucleotide terminal transferase-like activity. Similarly, the ability of permeabilized cells to incorporate radiolabeled CTP as well as UTP into TCA-precipitable material suggests that the polymerase activity we are detecting is not due to the polyuridylate polymerase present in the cytoplasm of mammalian cells (Hayashi and McFarlane, 1979).

Protease inhibitors and RNase inhibitors have both been reported to increase the RNA-dependent RNA polymerase activity present in extracts of West Nile virus-infected cells (Grun and Brinton, 1986). We therefore determined the effect of adding PMSF or aprotinin, two protease inhibitors, on the ability of permeabilized MHV-infected cells to direct the synthesis of actinomycin D-resistant RNA. As shown in Table 1, 50 μM PMSF decreased incorporation of CTP into TCA-precipitable RNA by about 20%. However, aprotinin increased activity by about 20%. We attribute the different effects of these compounds to the much broader spectrum of activity of PMSF, a drug which inhibits most serine esterases (Fahrney and Gold, 1963; Laskowski and Sealock, 1972). Surprisingly, the addition of placental RNase inhibitor had little effect on RNA synthesis by permeabilized cells.

The effect of ouabain on the MHV polymerase/permeabilized cell system was investigated because of the dependence of the system on an exogenous energy source. Ouabain is an inhibitor of the Na^+/K^+-dependent ATPase present in the plasma membrane (Ruoho and Kyte, 1974). We reasoned that after permeabilization this enzyme might be competing with the MHV polymerase complex for ATP. If this hypothesis is true we felt that the addition on an inhibitor of the ATPase to the system might stimulate the MHV polymerase activity. This did appear to be the case. Ouabain at concentrations of 1 and 20 ng/ml increased the polymerase activity to 125 and 131% of that observed in controls. We could not increase the concentration of ATP above 1 m*M* to directly test the idea that ouabain exerted its stimulatory effect on MHV polymerase activity by increasing the biologically effective ATP concentration in our reaction since concentrations of ATP greater than 1 m*M* caused the permeabilized cells to detach from the substrate and subsequently disintegrate. We therefore included ouabain at 1 ng/ml and aprotinin at 0.24 TIU/ml in all subsequent experiments.

Characterization of the products synthesized in permeabilized cells

The TCA-precipitable material synthesized in MHV-infected permeabilized cells was identified as RNA by its sensitivity to RNase. It was not sensitive to DNase (Table 2). To further characterize the RNA synthesized in our system, we extracted RNA from permeabilized

cells labeled with [α-^{32}P]CTP and from parallel cultures of intact MHV-infected cells labeled with [^{32}P]orthophosphate in the presence of actinomycin D. These samples were then analyzed by electrophoresis on a formaldehyde gel. The autoradiograph shown in Fig. 3 illustrates that the relative amounts and sizes of the RNA species synthesized in the permeabilized cells is very similar to the MHV-specific RNAs observed in intact cells.

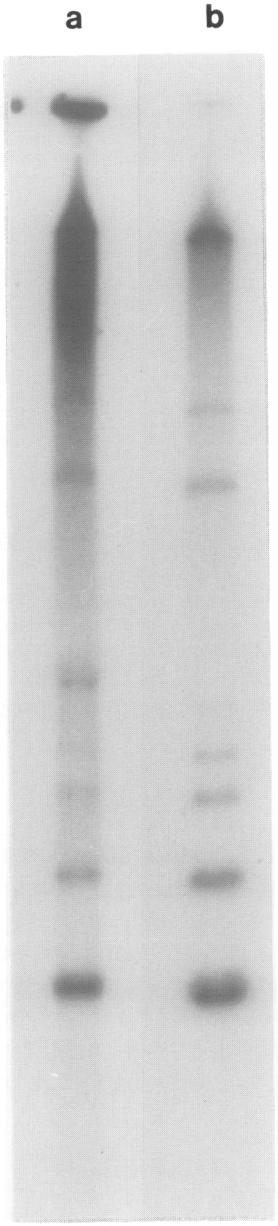

FIG. 3. Gel analysis of RNA products synthesized in permeabilized cells. Cells were infected with MHV-A59, incubated until 8.5 hr post-infection, and permeabilized. Permeabilized cells were labeled with [α-^{32}P]UTP, 250 μCi/ml, under our standard conditions for 40 min and the RNA was extracted (lane a). A replicate culture was not permeabilized but rather the intact cells were labeled with 500 μCi/ml[^{32}P]orthophosphate in the presence of actinomycin D for 40 min (lane b). The RNA samples were electrophoresed on an 0.8% agarose gel containing formaldehyde and autoradiographed.

Further evidence of the virus-specific nature of these RNAs was obtained by Southern blot hybridization. MHV-specific plasmid clones and a plasmid clone derived from the unrelated malignant rabbit fibroma virus were digested with the appropriate restriction enzyme to excise the cloned insert and resolved by agarose gel electrophoresis. The band at approximately 3.0 kbp (Fig. 4A, lane a) represents the cloning vector pGEM-1. The band at approximately 4.3 kbp (Fig. 4A, lanes b–e) represents pBR322. The band at approximately 2.8 kbp (Fig. 4A, lane f) represents pUC19. Replicate filters of molecular clones representing the most 3′ 10 kb of the MHV genome were hybridized with either random-primed cDNA synthesized from a purified virion RNA template (Fig. 4B), RNA extracted from MHV-infected permeabilized cells labeled with [α-^{32}P]UTP after permeabilization (Fig. 4C), or RNA prepared from mock-infected permeabilized cells. As expected, the random-primed cDNA probe hybridized to all of the MHV-specific clones (lanes a–e) and did not recognize the plasmid containing the malignant rabbit fibroma virus *Bam*HI fragment K (lane f). The labeled RNA synthesized after permeabilization of infected cells also hybridized specifically with the MHV inserts, although it did not give as strong a signal as random-primed cDNA probe (Fig. 4C). The apparent band at about 3.7 kbp in Panel C, lane e, as artifactual since no DNA is present at that position in the ethidium bromide stained gel. The signal with clones 118-8a and 414-8a was considerably weaker than the signal obtained with the other MHV-specific inserts. We attribute these differences in signal, at least in part, to the lower amount of these two inserts present in the gel (Fig. 4A). This is also reflected in the relative signals obtained with the random-primed probe. The specificity of the hybridization reaction was confirmed by the lack of hybridization of MHV-infected permeabilized reaction product with an irrelevant plasmid insert (Fig. 4C, lane g) and the failure of permeabilized cell reaction products from mock-infected cells to hybridize with these MHV clones (data not shown). Additionally, the extent of hybridization of the reaction products from permeabilized MHV-infected cells to MHV cDNA clones bound to nitrocellulose circles was similar to that of RNA prepared by labeling intact MHV-infected cells with [^{32}P]orthophosphate in the presence of actinomycin D (data not shown).

Kinetics of synthesis

The time course of incorporation of label in permeabilized cells was determined by preparing replicate

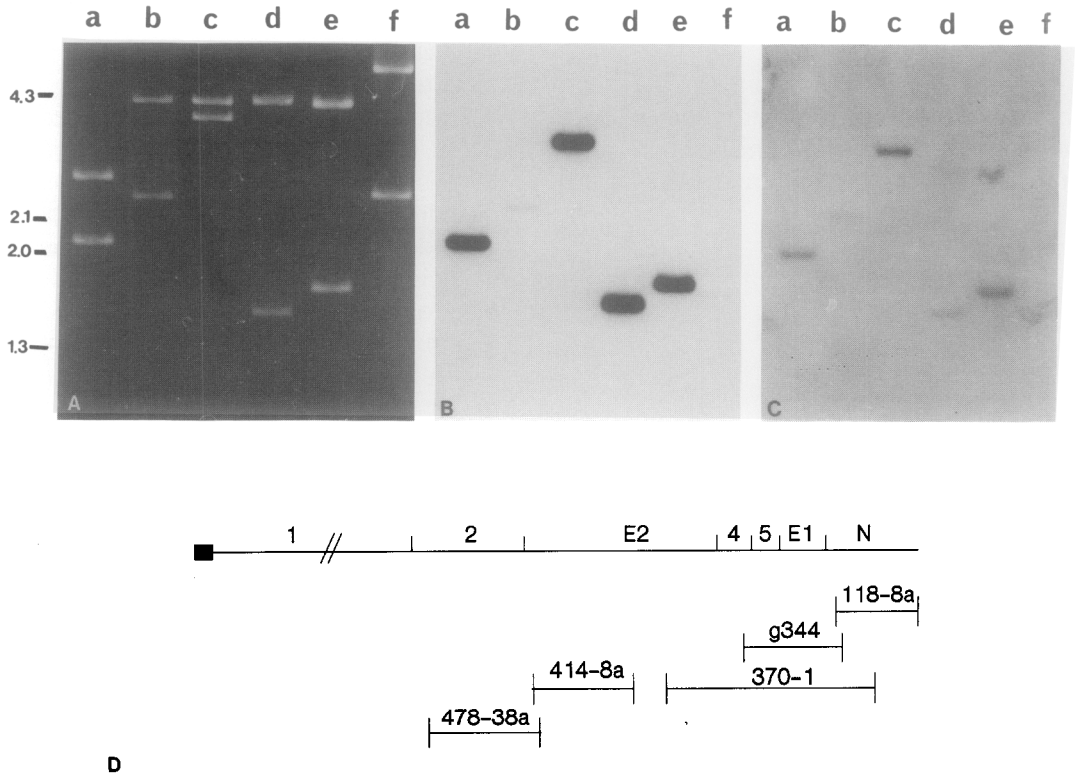

FIG. 4. Hybridization of RNA products of permeabilized MHV-infected cells to MHV-specific plasmid clones. Purified plasmid DNA was digested with *Pst*I, plasmids 478-38a (lane a), 414-8a (lane b), 370-1 (lane c), 118-8a (lane d), and g344 (lane e), or *Bam*HI in the case of the cloned malignant rabbit fibroma virus *Bam*HI fragment K (lane f). Replicate samples of the restriction digests were resolved by electrophoresis in a 1% agarose gel. (A) The pattern obtained by ethidium bromide staining. The positions of molecular weight markers, a *Hin*dIII digest of λ DNA, are indicated to the right of the photograph. (B) After Southern transfer to a nitrocellulose filter the DNA was hybridized to a random-primed MHV-A59 cDNA probe. The autoradiograph was exposed for 7 hr. (C) A replicate filter to that shown in (B) was hybridized to RNA synthesized in permeabilized MHV-A59-infected cells incubated with [α-^{32}P]CTP after permeabilization. The autoradiograph was exposed for 72 hr. (D) A schematic showing the approximate map positions of the MHV clones used in this experiment. The filled rectangle represents the MHV leader sequence at the 5′ end of the genome.

cultures of MHV-infected and mock-infected cells, incubating them for 8.5 hr, permeabilizing them using the standard conditions we had developed, and labeling them for the times indicated in Fig. 5. The accumulation of radioactivity in TCA-precipitable products increases, although not in a linear fashion, over the first 40 min of labeling. After that time the amount of TCA-precipitable radioactive product in the cells decreases dramatically.

The kinetics of the development of the MHV-specific RNA polymerase activity over the course of infection was determined in permeabilized cells. As shown in Fig. 6, the accumulation of MHV RNA polymerase activity in infected cells (Panel A), as detected by our assay, faithfully mirrored the kinetics of actinomycin D-resistant, [^{3}H]uridine incorporation into TCA-precipitable material (Panel B) during a series of 1-hr pulses. Polymerase activity is first detectable at 5 hr postinfection in these experiments. Subsequent experiments showed that the peak level of polymerase activity in permeabilized cells occurred at 11 hr postinfection (data not shown). Similar experiments with MHV-JHM yielded similar results, although polymerase activity appeared 1 hr later than during MHV-A59 infection. It should be noted that the infection proceeded somewhat slower in the experiments reported here than in our previously reported work (Leibowitz *et al.*, 1981). The reasons for this discrepancy are not known at this time.

DISCUSSION

In this work we report the development and characterization of a permeabilized cell system for assaying MHV-specific RNA polymerase activity. This activity was characterized as to its requirements for mono- and divalent cations, requirements for an exogenous energy source, pH optimum, and its time of appearance during the course of infection. The RNA products synthesized in permeabilized cells were demonstrated to be MHV-specific by agarose gel electrophoresis.

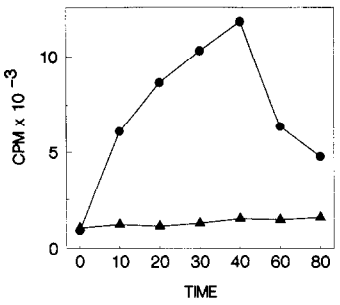

FIG. 5. The kinetics of incorporation of [^{3}H]CTP into MHV-specific RNA in permeabilized cells. Cells were infected with MHV-A59 (●) or mock-infected (▲), incubated until 8.5 hr postinfection, and permeabilized. Replicate cultures were incubated in buffer B containing 62.5 μCi/ml of [^{3}H]CTP under standard reaction conditions (Materials and Methods) for 0, 10, 20, 40, 60, and 80 min. At these times the cells were solublized and the amount of radioactive precursor incorporated into TCA-precipitable material was determined.

The purpose of the present work was to develop and characterize a system for studying the MHV-specific RNA polymerase that was more amenable to experimental manipulations than intact cells. To avoid difficulties in reproducing *in vitro* the intracellular environment which evolves during MHV infection we elected to pursue a path which would leave as much of the cell machinery in place as possible. The system we have developed has several advantages when compared to the cell-free systems developed by other workers. Although it is difficult to compare the relative efficiencies of different systems due to the different ways in which the experimental results have been presented, we can calculate the amount of RNA synthesized in our system. Using the optimized reaction conditions, one 35-mm well of MHV-infected permeabilized cells incorporated about 900 fmol of UMP into MHV-specific RNA. This is estimated to be about fivefold more RNA synthesis on a per cell basis than that obtained from a cell-free extract prepared from permeabilized cells (Compton *et al.*, 1987). Other workers using cell-free systems have reported yields on the basis of femtomoles of UMP/h/mg protein (Dennis and Brian, 1982; Mahey *et al.*, 1983; Brayton *et al.*, 1982, 1984). These have been in the range of 150–400 fmol/hr/mg protein. One 35-mm well of MHV-infected 17CL-1 cells contains about 450 μg of protein, providing a yield on a per milligram basis which is approximately 1800 fmol of UMP/mg protein/40 min, a figure which makes it at least four times more efficient than the previously described cell-free systems. There are no data at this time to suggest that our system, or any other MHV polymerase assay, is capable of initiating the synthesis of new strands of RNA.

A second advantage of permeabilized cells for studying MHV RNA synthesis is that the products synthesized accurately reflect the RNA species synthesized in intact MHV-infected cells. All seven of the MHV mRNA species are made in approximately the same ratios as they are *in vivo*. This contrasts with truly cell-free systems in which the RNA products synthesized were not characterized as to the precise molecular species of RNA synthesized (Brayton *et al.*, 1982, 1984; Mahey *et al.*, 1983), or those in which the major product was genome length (Compton *et al.*, 1987). Although the reasons for this difference in the RNA products synthesized are unknown, a possible explanation for this observation is the loss of a soluble factor responsible for regulating MHV transcription during preparation of cell-free extracts. Other explanations are possible as well, and additional work is needed to identify putative factors needed for the appropriate regulation of MHV RNA synthesis.

The kinetics of the accumulation of polymerase activity we observed parallels the increase of actinomycin D-resistant uridine incorporation which occurs during MHV infection. No early peak of polymerase activity or uridine incorporation in intact cells was detected. In this regard our results are similar to those of Compton *et al.* (1987) and Sawicki and Sawicki (1986). These results differ from those of earlier workers (Brayton *et al.*, 1982, 1984) who detected a peak of polymerase activity at 2 hr postinfection followed by a fall in activity prior to a subsequent increase to maximal levels. The reasons for these differences is not known. It could relate to the different cell lines used by different laboratories

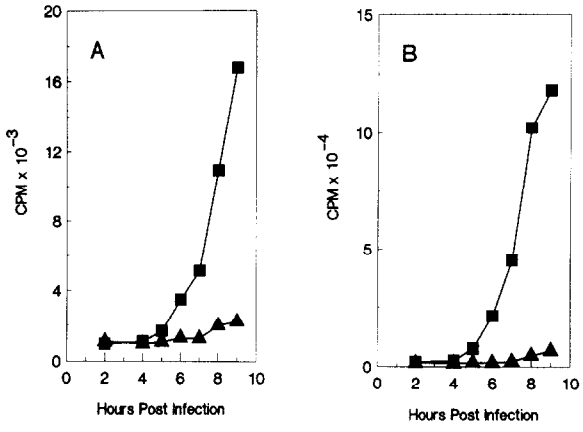

FIG. 6. The accumulation of MHV-specific RNA polymerase activity during infection. Replicate cultures of 17Cl-1 cells were infected with MHV-A59 (■) or mock-infected (▲) and incubated for 2 hr. At that time, and at hourly intervals thereafter, duplicate sets of cultures were either permeabilized and assayed for the incorporation of radioactive CTP into TCA-precipitable material under standard reaction conditions (A) or exposed to actinomycin D (5 μg/ml) for 15 min and labeled with 100 μCi of [^{3}H]uridine for 1 hr and then solublized with SDS and assayed for incorporation of label into TCA-precipitable material (B).

or be related to the vastly different reaction conditions that are employed by the different methods of assaying MHV polymerase activity.

The system we have described for assaying the MHV-induced RNA-dependent RNA polymerase activity should prove useful for other workers. It is simple to set up, provides a system which should be amenable to pulse–chase-type experiments, and furnishes a system where macromolecules such as RNA templates or purified proteins can be added and their effect on MHV synthesis observed. It may also serve as a point of departure for developing a completely cell-free system which better reflects the intracellular synthesis of MHV RNAs than the currently available systems.

ACKNOWLEDGMENTS

This work was supported by Public Health Service Grant NS 20834 from the National Institute of Neurologic and Communicative Diseases and Stroke. The authors thank Dr. Mark Schoenberg for performing some of the preliminary work which inspired us to continue these experiments and Dr. Emelia Oleszak for a thoughtful reading of the manuscript.

REFERENCES

BARIC, R. S., STOHLMAN, S. A., RAZAVI, M. K., and LAI, M. M. C. (1985). Characterization of leader-related small RNAs in coronavirus-infected cells: Further evidence for leader-primed mechanism of transcription. *Virus Res.* **3,** 19–33.

BOURSNELL, M. E. G., BROWN, T. D., FOULDS, I. J., GREEN, P. F., TOMLEY, F. M., and BINNS, M. M. (1987). Completion of the sequence of the genome of the coronavirus avian infectious bronchitis virus. *J. Gen. Virol.* **68,** 57–77.

BRAYTON, P. R., LAI, M. M. C., PATTON, C. D., and STOHLMAN, S. A. (1982). Characterization of two RNA polymerase activities induced by mouse hepatitis virus. *J. Virol.* **42,** 847–853.

BRAYTON, P. R., STOHLMAN, S. A., and LAI, M. M. C. (1984). Further characterization of mouse hepatitis virus RNA-dependent RNA polymerases. *Virology* 133, 197–201.

BUDZILOWICZ, C. J., WILCZYNSKI, S. P., and WEISS, S. R. (1985). Three intragenic regions of coronavirus mouse hepatitis virus strain A59 genome RNA contain a common nucleotide sequence that is homologous to the 3′ end of the viral mRNA leader sequence. *J. Virol.* **53,** 834–840.

CABIRAC, G. F., MULLOY, J. J., STRAYER, D. S., SELL, S., and LEIBOWITZ, J. L. (1986). Transcriptional mapping of early RNA from regions of the genome of the Shope fibroma and malignant rabbit fibroma virus genomes. *Virology* **153,** 53–69.

CHELEY, S., ANDERSON, R., CUPLES, M. J., LEE CHAN, E. C. M., and MORRIS, V. L. (1981). Intracellular murine hepatitis virus virus-specific RNAs contain common sequences. *Virology* **112,** 596–604.

COMPTON, S. R., ROGERS, D. B., HOLMES, K. V., FERTSCH, D., REMENICK, J., and MCGOWAN, J. J. (1987). *In vitro* replication of mouse hepatitis virus strain A59. *J. Virol.* **61,** 1814–1820.

CONDRA, J. H., and LAZZARINI, R. A. (1980). Replicative RNA synthesis and nucleocapsid assembly in vesicular stomatitis virus-infected permeable cells. *J. Virol.* **36,** 796–804.

DENISON, M. R., and PERLMAN, S. (1986). Translation and processing of mouse hepatitis virus virion RNA in a cell-free system. *J. Virol.* **60,** 12–18.

DENISON, M., and PERLMAN S. (1987). Identification of putative polymerase gene product in cells infected with murine coronavirus A59. *Virology* **157,** 565–568.

DENNIS, D. E., and BRIAN, D. A. (1982). RNA-dependent RNA polymerase activity in coronavirus-infected cells. *J. Virol.* **42,** 153–164.

FAHRNEY, D. E., and GOLD, A. M. (1963). Sulfonylfluorides. I. Rates of reaction with acetylcholinesterases, α-chymotrypsin and trypsin. *J. Amer. Chem. Soc.* **85,** 997–1003.

GRUN, J. B., and BRINTON, M. A. (1986). Characterization of West Nile virus RNA-dependent RNA polymerase and cellular terminal adenylyl and uridylyl transferases in cell-free extracts. *J. Virol.* **60,** 1113–1124.

HAYASHI, T. T., and MCFARLANE, K. (1979). Comparison of endogenous and exogenous RNA primers of poly(U) polymerase in rat hepatic ribosomes. *Biochem. J.* **177,** 895–902.

LAI, M. M. C., BARIC, R. S. BRAYTON, P. R., and STOHLMAN, S. A. (1984). Characterization of leader RNA sequences on the virion and mRNAs of mouse hepatitis virus, a cytoplasmic RNA virus. *Proc. Natl. Acad. Sci. USA* **81,** 3626–3630.

LAI, M. M. C., BRAYTON, P. R., ARMEN, R. C., PATTON, C. D., PUGH, C., and STOHLMAN, S. A. (1981). Mouse hepatitis virus A59: mRNA structure and genetic localization of the sequence divergence from hepatotropic strain MHV-3. *J. Virol.* **39,** 823–834.

LAI, M. M. C., PATTON, C. D., BARIC, R. S., and STOHLMAN, S. A. (1983). Presence of leader sequences in the mRNA of mouse hepatitis virus. *J. Virol.* **46,** 1027–1033.

LAI, M. M. C., PATTON, C. D., and STOHLMAN, S. A. (1982a). Further characterization of mRNAs of mouse hepatitis virus: Presence of common 5′-end nucleotides. *J. Virol.* **41,** 557–565.

LAI, M. M. C., PATTON, C. D., and STOHLMAN, S. A. (1982b). Replication of mouse hepatitis virus: Negative stranded RNA and replicative form RNA are of genome length. *J. Virol.* **44,** 487–492.

LASKOWSKI, M., and SEALOCK, R. W. (1972). Protein protease inhibitors–Molecular aspects. *In* "The Enzymes," 3rd ed. (P. D. Boyer, Ed.), pp. 375–473. Academic Press, New York.

LEIBOWITZ, J. L., WEISS, S. R., PAAVOLA, E., and BOND, C. W. (1982). Cell-free translation of murine coronavirus RNA. *J. Virol.* **43,** 905–913.

LEIBOWITZ, J. L., WILHELMSEN, K. C., and BOND, C. W. (1981). The virus-specific intracellular RNA species of two murine coronaviruses: MHV-A59 and MHV-JHM. *Virology* **114,** 39–51.

LERACH, H., DIAMOND, D., WOZNEY, J. M., and BOEDTKER, H. (1977). RNA molecular weight determinations of gel electrophoresis under denaturing conditions, a critical reexamination. *Biochemistry* **96,** 4743–4751.

LOMNICZI, B. (1977). Biological properties of avian coronavirus RNA. *J. Gen. Virol.* **36,** 531–533.

MAHEY, B. W. J., SIDDELL, S., WEGE, H., and TER MEULEN, V. (1983). RNA-dependent RNA polymerase activity in murine coronavirus-infected cells. *J. Gen. Virol.* **64,** 103–111.

ROBB, J. A., and BOND, C. W. (1979). Pathogenic murine coronaviruses. I. Characterization of biologic behavior *in vitro* and virus-specific intracellular RNA of strongly neurotropic JHMV and weakly neurotropic A59V viruses. *Virology* **94,** 352–370.

RUOHO, A., and KYTE, J. (1974). Photoaffinity labeling of the ouabain-binding site on (Na^+ + K^+) adenosine triphosphatase. *Proc. Natl. Acad. Sci. USA* **71,** 2352–2356.

SAWICKI, S. G., and SAWICKI, D. L. (1986). Coronavirus minus-strand RNA synthesis and effect of cycloheximide on coronavirus RNA synthesis. *J. Virol.* **57,** 328–334.

SCHMIDT, I., SKINNER, M., and SIDDELL, S. (1987). Nucleotide sequence of the gene encoding the surface projection glycoprotein of coronavirus MHV-JHM. *J. Gen. Virol.* **68,** 47–56.

SOUTHERN, E. M. (1975). Detection of specific sequences among DNA fragments separated by gel electrophoresis. *J. Mol. Biol.* **98,** 503–518.

SPAAN, W. J., DELIUS, H., SKINNER, M., ARMSTRONG, J., ROTTIER, P., SMEEKENS, S., VAN DER ZEIJST, B. A. M., and SIDDELL, S. G. (1983). Coronavirus mRNA synthesis involves fusion of non-contiguous sequences. *EMBO J.* **2,** 1839–1844.

SPAAN, W. J., ROTTIER, P. J., HORZINEK, M. C., and VAN DER ZEIJST, B. A. M. (1981). Isolation and identification of virus-specific mRNAs in cells infected with mouse hepatitis virus (MHV-A59). *Virology* **108,** 424–434.

SPAAN, W. J., ROTTIER, P. J., HORZINEK, M. C., and VAN DER ZEIJST, B. A. (1982). Sequence relationships between the genome and the intracellular RNA species 1, 3, 6, and 7 of mouse hepatitis virus strain A59. *J. Virol.* **42,** 432–439.

STERN, D. F., and KENNEDY, S. I. T. (1980a). Coronavirus multiplication strategy. I. Identification and characterization of virus-specified RNA. *J. Virol.* **34,** 665–674.

STERN, D. F., and KENNEDY, S. I. T. (1980b). Coronavirus multiplication strategy. II. Mapping the avian infectious bronchitis virus intracellular RNA species to the genome. *J. Virol.* **36,** 440–449.

STRAYER, D. S., CABIRAC, G. F., SELL, S., and LEIBOWITZ, J. L. (1983b). Malignant rabbit fibroma virus: Observations on the culture and histopathologic characteristics of a new virus-induced rabbit tumor. *J. Natl. Cancer Inst.* **71,** 91–104.

STRAYER, D. S., SKALETSKY, E., CABIRAC, G. F., SHARP, P. A., CORBEIL, L. B., SELL, S., and LEIBOWITZ, J. L. (1983a). Malignant rabbit fibroma virus causes secondary immunosupression in rabbits. *J. Immunol.* **130,** 399–404.

STURMAN, L. S., and TAKEMOTO, K. K. (1972). Enhanced growth of a murine coronavirus in transformed mouse cells. *Infect. Immun.* **6,** 501–507.

WEISS, S. R., and LEIBOWITZ, J. L. (1983). Characterization of murine coronavirus RNA by hybridization with virus-specific cDNA probes. *J. Gen. Virol.* **64,** 127–133.

WITTEK, R., HANGGI, M., and HILLER, G. (1984). Mapping of a gene coding for a major late structural polypeptide on the vaccinia virus genome. *J. Virol.* **49,** 371–378.

YOGO, Y., HIRANO, N., HINO, S., SHIBUTA, H., and MATUMOTO, M. (1977). Polyadenylate in the virion RNA of mouse hepatitis virus. *J. Biochem.* **82,** 1103–1108.